Resilience Oriented Planning of Urban Multi-Energy Systems With Generalized Energy Storage Sources

Wujing Huang, *Student Member, IEEE*, Xi Zhang, *Member, IEEE*, Kangping Li, *Member, IEEE*, Ning Zhang, *Senior Member, IEEE*, Goran Strbac, *Member, IEEE*, and Chongqing Kang, *Fellow, IEEE*

***Abstract*—In the last decade, a number of severe urban power outages have been caused by extreme natural disasters, e.g., hurricanes, snowstorms and earthquakes, which highlights the need for rethinking current planning principles of urban energy systems and expanding the classical reliability-oriented view. In addition to being reliable to low-impact and high-probability outages, power system should also have high level of resilience to withstand high-impact and low-probability (HILP) events. Compared with power system, multi-energy systems (MESs) have advantages in improving resilience through energy shifting across multiple energy sectors, a variety of generalized energy storage resources and thermal inertia of heat/cooling loads. This paper proposes a resilience-oriented planning method to determine optimal configuration of distribution level MES, e.g., urban energy supply systems, considering comprehensive impacts from supply, network and demand sides in MES. Impacts of energy shifting at supply side, pipe storage at network side and thermal inertia at demand side are described in the same linear modeling framework using energy hub (EH) model. Generalized energy storage resources including centralized and distributed energy storage devices, pipe network storage and building heat capacity are all modeled into centralized energy storage to facilitate an efficient configuration planning of MES.**

***Index Terms*—Configuration planning, energy hub, energy storage, gas network, heat network, multi-energy systems, resilience assessment, thermal inertia.**

I. Introduction

THE planning and operation of power systems traditionally conform to reliability requirement, e.g., "N-1" security principle, to withstand low impact, high probability, more predictable and more credible power outages [1]. In the last decade, a number of severe power outages have been caused by extreme natural disasters, e.g., hurricanes, floods and ice storms, which highlights the need for rethinking current planning principles and expanding the classical reliability-oriented view [2]. In contrast to typical power system outages, the natural disaster related events have the characteristics of high impact and low probability. Multiple component failures can simultaneously happen in an extreme natural disaster and there is usually a spatiotemporal correlation between these failures [3]. In addition to being reliable to low-impact and high-probability outages, power system should also have high level of resilience to withstand high-impact and low-probability (HILP) events. Resilience is defined as the ability to anticipate, withstand, adapt to and recover from an HILP and extraordinary event [4].

In power systems, at any one time, the amount of power consumed by the loads must equal the amount of power produced by the supplies less the power lost in transmission. This characteristic of instantaneous power balance brings great difficulty to continuous power supply when an HILP event happens. Moreover, the flexibility of energy supply within one single energy sector is relatively limited, which further limits the resilience of the energy supply infrastructures. In recent years, multi-energy systems (MES) have been paid much attention to in more and more research and practices, aiming to obtain greater economic, environmental and security benefits in integrated energy systems besides power systems. In MES, multiple energy sectors, e.g., electricity, gas, heat and cooling, interact with each other by energy conversion, enabling the energy shifting across different energy sectors [5]. Compared with "classical" energy system, including power system, in which energy sectors are treated independently, MES has three main advantages in improving resilience: 1) The flexibility of energy supply is unlocked because energy shifting across multiple energy sectors is realized by various types of energy converters in MES. The impact of a failure that happens in an energy sector in MES can be resisted and absorbed by another or multiple energy sectors. 2) A variety of centralized, distributed and equivalent energy storage resources provide adequate reserve during HILP events. Compared to battery, hot water and gas tanks are more economical and practical ways to store energy. In particular, the hot water and gas pipes in heat and gas networks store considerable energy, which can continue to be used during a certain time period after the heat and gas sources fail. 3) The thermal inertia of heat load, e.g., space heating for buildings, relaxes the constraint of instantaneous power balance. With the disconnection of heat

Manuscript received May 2, 2021; revised September 1, 2021; accepted October 17, 2021. Date of publication October 27, 2021; date of current version June 20, 2022. This work was supported in part by the International (Regional) Joint Research Project of National Natural Science Foundation of China under Grant 52061635101 and in part by Tsinghua University Initiative Scientific Research Program under Grant 20193080026. Paper no. TPWRS-00686-2021. *(Corresponding authors: Ning Zhang; Chongqing Kang.)*

Wujing Huang, Kangping Li, Ning Zhang, and Chongqing Kang are with the State Key Lab of Power Systems, Department of Electrical Engineering, Tsinghua University, Beijing 100084, China, and also with the International Joint Laboratory on Low Carbon Clean Energy Innovation, Beijing 100084, China (e-mail: 163.com.hwj@163.com; kangpingli@mail.tsinghua.edu.cn; ningzhang@tsinghua.edu.cn; cqkang@tsinghua.edu.cn).

Xi Zhang and Goran Strbac are with the Department of Electrical and Electronic Engineering, Imperial College London, London SW7 2AZ, U.K. (e-mail: x.zhang14@imperial.ac.uk; g.strbac@imperial.ac.uk).

Color versions of one or more figures in this article are available at https://doi.org/10.1109/TPWRS.2021.3123074.

Digital Object Identifier 10.1109/TPWRS.2021.3123074

supply, it will take some time for the indoor temperature to change from the set-point to an unacceptable value [6]. The user experience will not be greatly affected in a certain time after the failure of heat supply, which provides a buffer for the impact of HILP events.

Massive research has been dedicated to studying the resilience of power systems. These studies mainly focus on two categories of problems, i.e., resilience assessment and resilience improvement. Different types of metrics have been proposed to quantify the operational and infrastructure resilience of power systems [7], [8]. A relatively comprehensive framework of resilience assessment of power systems is presented in [9]. The resilience improvement measures of power systems are divided into two categories, i.e., operational measures and hardening measures. Operational measures are further divided into preventive, corrective and restorative categories. Preventive measures aim to accurately anticipate and prepare for HILP events before they happen. The literature of preventive categories mainly focuses on natural disaster forecasting [10], day-ahead unit commitment [11], [12], resource pre-allocation [13] and network topology switching [14]. Corrective measures aim to withstand and effectively adapt to unfolding HILP events. The literature of corrective categories mainly focuses on resiliency-oriented operation strategy [15], network topology reconfiguration (particularly sectionalization into microgrids) [16] and demand response [17]. Restorative measures aim to rapidly recover after HILP events. The literature of restorative categories mainly focuses on networked microgrid aiding [18], repair crew dispatch [19], mobile power sources (e.g., mobile generators) dispatch [20] and the integration of these measures [21]. Hardening measures, or planning measures, aim to reinforce the system infrastructure prior to HILP events and guarantee the resiliency-oriented operation. In transmission level, resiliency-oriented line hardening is mostly studied [22]. The allocation of distributed generators is also considered besides line hardening in distribution level planning problems [23]. The planning of energy storage devices, which are regarded as important resilience resources, is also studied by researchers [24].

Current research on the resilience of MES is also categorized into two main groups, i.e., resilience assessment of MES and resilience improvement of MES. Monte Carlo (MC) simulation method is mainly used to assess the resilience of MES. A number of HILP event scenarios or their resulting system outage scenarios are sequentially sampled. The load shedding minimization problem is iteratively solved for each sampled scenario until the resilience indices meet the stopping criterion [25], [26]. Similarly, the resilience improvement of MES is studied from either operational perspective or hardening perspective. The literature of operational measures mainly focuses on proactive scheduling [27], [28], unit commitment [29] and repair crew dispatch [30]. The literature of hardening measures of MES is further divided into transmission level and distribution level categories. In transmission level MES, the energy transmission characteristic of multiple energy networks is the main concern; therefore, current research mainly focuses on the optimization of line hardening strategy or expansion planning strategy for integrated power and gas transmission networks. As for the methodology, the tri-level (defender-attacker-defender) robust optimization technique, where the upper level determines optimal network hardening strategy, the middle level identifies maximum damage of MES caused by HILP events and the lower level explores reaction for minimizing load shedding in response to HILP events, is mostly used in current research, e.g., [31], [32] and [33]. The main concern of distribution level MES is energy conversion and shifting across multiple energy sectors. Some research has made contributions in proposing methodology to improve the resilience of energy conversion configuration of distribution level MES. Reference [34] proposed a genetic algorithm-based planning method considering resilient scheduling to generate a more reasonable configuration of distribution level MES for the operation resilience against supply side outages. Reference [35] proposed a resilience-oriented configuration planning method for distribution level MES considering the interaction of demand response, e.g., adjustable load and interruptible load.

The transmission level MES, e.g., integrated power and gas transmission networks, has a relatively weaker coupling among different energy sectors and its resilience analysis is similar to that of separate energy networks. While the distribution level MES, e.g., urban energy supply systems, where multiple energy sectors greatly interact with others by various types of energy convertors, brings several new problems to its resilience analysis and planning compared to those of power system:

1) Impacts of energy shifting at supply side. Power system resilience analysis is mainly based on the accurate model of power system itself. For MES, the energy conversion configuration should also be accurately modeled to study how a failure that happens in an energy sector influences the rest energy sectors, and whether the impact of this failure can be resisted and absorbed by another or multiple energy sectors.
2) Impacts of pipe network storage at network side. In power system, batteries and standby generators are used to provide emergency power supply during HILP events. In MES, the considerable amount of energy stored in the heat and gas pipe networks can continue to be used after the energy sources fail. Therefore, besides more kinds of energy storage devices and standby units, the pipe network storage should also be considered for emergency supply.
3) Impacts of load thermal inertia at demand side. Power system operation has the characteristic of instantaneous power balance of supply and demand. In MES, the thermal inertia of heat/cooling load relaxes the constraint of instantaneous power balance. The lag between the failure of energy supply and load shedding, which offers a buffer for MES to effectively survive a HILP event, should be considered in the resilience analysis and planning.

However, current research on the resilience of distribution level MES mainly considers the first point, i.e., energy shifting, in the planning or operation model. The resilience resources in the gas, heat and cooling sectors, besides the electricity sector, are not fully utilized to support the resilience-oriented planning of MES. To fill this gap in the research on resilience of MES, this paper proposes a planning method to determine the optimal configuration of distribution level MES considering the

comprehensive impacts from supply, network and demand sides in MES. To avoid directly embedding the nonlinear models of pipe network and heat/cooling load in the planning model, the pipe network storage and load thermal inertia are modeled as generalized energy storage sources in the proposed method. The contribution of this paper is twofold:

1) A resilience-oriented planning method to determine optimal configuration of distribution level MES is proposed. Resilience resources from supply, network and demand sides in MES are all taken into consideration to support the resilient energy supply of MES in HILP events of different intensities.
2) A generalized energy storage model is proposed to facilitate an efficient resilience-oriented planning of energy resources in MES. The impacts of energy shifting at supply side, pipe storage at network side and thermal inertia at demand side are described in the same linear modeling framework using energy hub (EH) model.

The remainder of the paper is structured as follows. Section II presents the basic models that are used in the proposed planning method, including the proposed generalized energy storage model. Section III presents the proposed resilience-oriented planning method of distribution level MES. Section IV conducts a case study of planning of distribution level MES using the proposed resilience-oriented planning method. Section V concludes the paper.

II. Model of Distribution Level MES

This section presents the basic models that are used in the proposed planning method, including model of energy conversion configuration of distribution level MES, model of pipe storage capacity, model of building thermal inertia, and probability model of component failure and repair.

A. Modeling Energy Conversion Configuration: Energy Bus-Based Energy Hub Model

In distribution level MES, various types of energy converters and energy storage devices together form an energy conversion configuration. The key of modeling distribution level MES is to accurately model the energy conversion relationship among different energy sectors. Prof. Andersson first proposed the concept of EH in 2007 [36] to model the steady-state energy conversion relationship across multiple energy sectors in MES [37]. The used EH model in this paper, i.e., energy bus-based EH model, is a variant of the original EH model. The energy bus-based EH model is first proposed in [38], aiming to facilitate the planning of configuration of distribution level MES. Fig. 1 presents a typical energy bus-based EH which models a distribution level MES purchasing electricity and natural gas from upper power and natural gas transmission networks and meeting electricity, heat and cooling demands.

Components of energy bus-based EH model are categorized into three groups, i.e., buses, nodes and branches. A bus is a junction that concentrates the energy flows from different sources upstream, e.g., energy converters, energy storage devices and energy networks outside EH, and distributes the total energy to downstream loads. The EH shown in Fig. 1 has four buses, i.e., electricity bus, natural gas bus, heat bus, and cooling bus. The buses can correspond to real facilities, e.g., transformers, natural gas gate stations and heat exchange stations. Nodes inside EH are equipment nodes representing different energy converters and energy storage devices. The EH shown in Fig. 1 has eight equipment nodes, i.e., combined heat and power unit (CHP), renewable energy source (RES), electric heat pump (EHP), auxiliary boiler (AB), heat storage device (HS), compression electric refrigerator group (CERG), water absorption refrigerator group (WARG), and cooling storage device (CS). Nodes outside EH are interface nodes representing external energy infrastructures and loads. The EH shown in Fig. 1 has four interface nodes, i.e., external power and natural gas transmission networks, electricity load, heat load, and cooling load. A branch, which represents a direction of energy flow, connects nodes to buses in EH. The EH shown in Fig. 1 has twenty-one branches. The CHP node is connected to natural gas bus, electricity bus and heat bus by three branches, which means that the CHP takes in natural gas from natural gas bus while supply electricity and heat to electricity bus and heat bus, respectively. A branch can also correspond to a real energy infrastructure, e.g., a power distribution network, a natural gas distribution network and a heat distribution network.

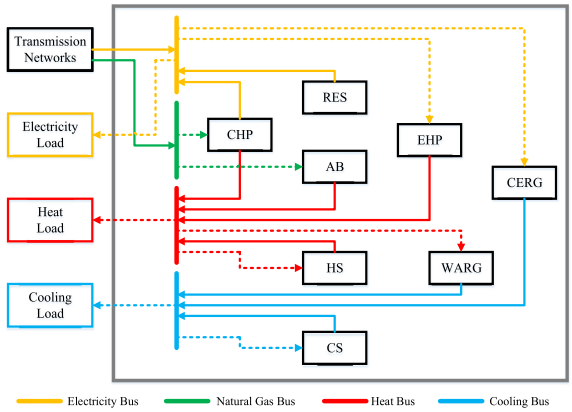

Fig. 1. A typical energy bus-based EH representing distribution level MES.

B. Modeling Discharging of Energy Stored in Pipe Network

In contrast to power networks, where electricity cannot be stored in lines, natural gas, heat and cooling networks always store a certain amount of energy in their pipelines during daily operation [39]. The energy stored in these pipelines can be adjusted by changing the pressure of gas in natural gas network or changing the temperature of water in heat/cooling network.

If a heat source fails and its downstream hot water pipelines survive in an HILP event, taking heat network as an example here, the heat stored in these pipelines would not immediately lose with the disconnection of heat source. As a result, the downstream hot water pipe network can be equivalent to a heat storage tank for emergency heat supply. The hot water pipe network discharges the stored heat like other real heat storage devices

until the temperature of water decreases to ambient temperature. The model of discharging of pipe network equivalent storage is:

$$E_l \cdot (SOC_l(t+1) - SOC_l(t)) = -P_l(t)/\eta_l \cdot \Delta t \quad (1)$$

where E_l is the energy capacity of equivalent storage of pipe network l, $SOC_l(t)$ is the state-of-charge of equivalent storage of pipe network l in t-th time period, $P_l(t)$ is discharging thermal power of equivalent storage of pipe network l in t-th time period, η_l is the discharging efficiency of equivalent storage of pipe network l, and Δt is the duration of one time period. E_l is equal to the stored heat of pipe network l at the onset of the HILP event:

$$E_l = c_p m_l \cdot (T_l(0) - T_a) \quad (2)$$

where c_p is the specific heat capacity of water, m_l is the mass of water held in pipe network l, $T_l(0)$ is the average temperature of water in pipe network l at the onset of the HILP event, and T_a is ambient temperature. Therefore, $SOC_l(0) = 1$ and SOC_l decreases to zero if the temperature of water in pipe network l decreases to ambient temperature:

$$0 \le SOC_l(t) \le 1, \forall t \quad (3)$$

P_l can be adjusted by controlling the volumetric flow rate of water in pipe network l to obtain an optimal discharge strategy. However, the energy stored in pipe network is considered to be unavailable if a failure happens in pipe network.

C. Modeling Thermal Inertia of Heat/Cooling Load

Electricity loads, e.g., lighting, in power system have no inertia toward the change of electricity supply, that is, these loads are unserved once the electricity supply fails. On the contrary, some heat/cooling loads, e.g., space heating/cooling for buildings, have thermal inertia toward the change of heat/cooling supply, that is, it takes some time for these loads to be unserved after the heat/cooling supply fails. This is because the comfort temperature for users has a certain zone and the user experience will not be significantly affected until the indoor temperature is beyond the comfort zone. This lag between the failure of energy supply and load shedding offers a buffer for MES to effectively survive a HILP event. The thermal inertia of heat load is illustrated in Fig. 2, where the heat supply fails at t_0, the indoor temperature leaves the comfort zone at t_{LS0}, the heat supply system is restored at t_{RS}, and the indoor temperature returns to the comfort zone at t_{LSe}. However, if the indoor temperature is away from the comfort zone before MES recovers from the HILP event, it will also take some time for the indoor temperature to return to the comfort zone after the energy supply repairs, as shown in Fig. 2. Therefore, the sign of MES recovery is not the restoration of energy infrastructures but the restoration of load supply.

Quantitatively, the model of space heating for a building is:

$$\begin{aligned} Q(t+1) - Q(t) &= C_b \cdot (T_b(t+1) - T_b(t)) \\ &= (P_{in}(t) - P_{load}(t)) \cdot \Delta t \end{aligned} \quad (4)$$

where $Q(t)$ is the heat stored in the interior space of building in t-th time period, C_b is the heat capacity of the interior space of building, $T_b(t)$ is the indoor temperature of building in t-th time period, $P_{in}(t)$ is the thermal power provided by heat supply system in t-th time period, and $P_{load}(t)$ is the heat load of building in t-th time period. In daily operation, $P_{in} = P_{load}$ and thus the indoor temperature of building keeps constant. When the heat supply fails, e.g., $P_{in} = 0$, (4) is rewritten as:

$$\begin{aligned} P_{load}(t) \cdot \Delta t &= P_{disch}(t) \cdot \Delta t \\ &= Q(t) - Q(t+1) = C_b \cdot (T_b(t) - T_b(t+1)) \end{aligned} \quad (5)$$

where $P_{disch}(t)$ is the equivalent discharging thermal power of the interior space of building in t-th time period. This equivalent discharging thermal power is equal to the decrease rate of the heat stored in the interior space of building, which is calculated according to the decrease of indoor temperature and the heat capacity of the interior space of building.

According to (5), the thermal inertia of heat/cooling load is modeled by an equivalent heat/cooling storage device, which begins to discharge thermal/cooling power to supply heat/cooling load when heat/cooling supply system fails to satisfy the required demand:

$$E_b \cdot (SOC_b(t+1) - SOC_b(t)) = -P_{disch}(t) \cdot \Delta t \quad (6)$$

where E_b and SOC_b are the energy capacity and state-of-charge of the equivalent storage device, respectively. Considering that the heat/cooling load is totally unserved when the indoor temperature is beyond the comfort zone, E_b here only models the temperature variation within the comfort zone:

$$E_b = C_b \cdot |T_b(0) - T_{\text{limit}}| \quad (7)$$

where $T_b(0)$ is the indoor temperature at the onset of the HILP event, and T_{limit} is the limit of comfort temperature (using lower limit for heat load while upper limit for cooling load).

Fig. 3 presents the equivalent of EH shown in Fig. 1 encountering a HILP event. The hot/cold water pipe network storage for emergency supply and the thermal inertia of heat load are considered. Three components in EH fail in this HILP event: 1) a node representing EHP, 2) a branch representing power distribution network between electricity bus and CERG, and 3)

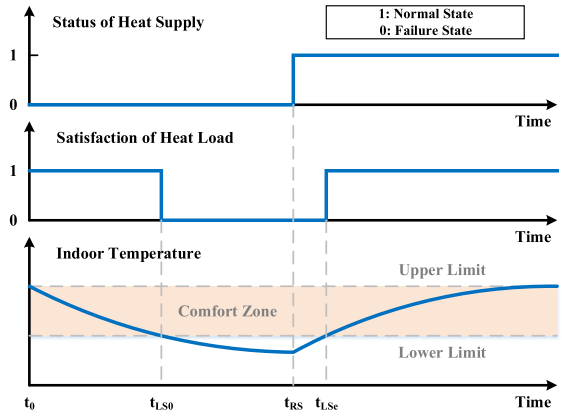

Fig. 2. Illustration of thermal inertia of heat load.

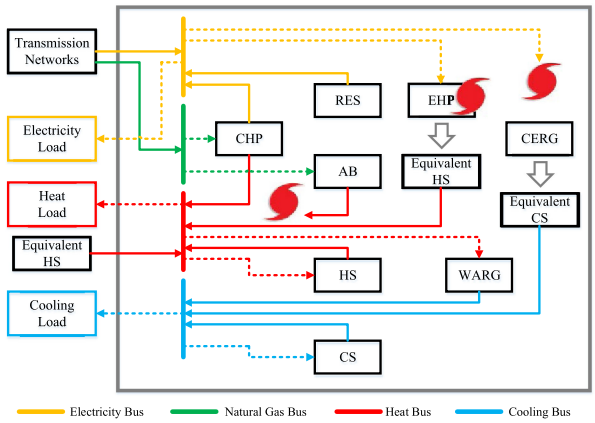

Fig. 3. Equivalent of EH shown in Fig. 1 encountering a HILP event and considering pipe network storage for emergency supply and thermal inertia of heat load.

TABLE I
SUMMARY OF PROPOSED GENERALIZED ENERGY STORAGE MODEL

Type	Formula	Main parameters & variables		
		E	P	η
Energy storage device	$E\cdot(SOC(t+1)-SOC(t))=-P/\eta\cdot\Delta t$	E_s	P_s	η_s
Pipe network storage		$c_p m_l\cdot(T_l(0)-T_a)$	P_l	η_l
Load thermal inertia		$C_b\cdot\lvert T_b(0)-T_{\text{limit}}\rvert$	P_{disch}	1

a branch representing heat distribution network between AB and heat bus. As shown in Fig. 3, the equivalent HS and CS inside EH are introduced to model the energy storage of pipe network in the downstream of EHP and CERG, respectively. While the heat stored in pipe network in the downstream of AB is unavailable. The equivalent HS outside EH is introduced to model the thermal inertia of heat load.

D. Summary of Generalized Energy Storage Model

For an energy storage device, e.g., battery and hot water tank, the model of its operation is:

$$E_s\cdot(SOC(t+1)-SOC(t))=-P_s/\eta_s\cdot\Delta t \tag{8}$$

where E_s is energy capacity of an energy storage device, P_s is discharging/charging power of an energy storage device (P_s is positive when discharging and negative when charging), and η_s is discharging/charging efficiency of an energy storage device.

According to (1) and (6), a generalized energy storage model is proposed:

$$E\cdot(SOC(t+1)-SOC(t))=-P/\eta\cdot\Delta t \tag{9}$$

The details of the proposed generalized energy storage model are summarized in Table I.

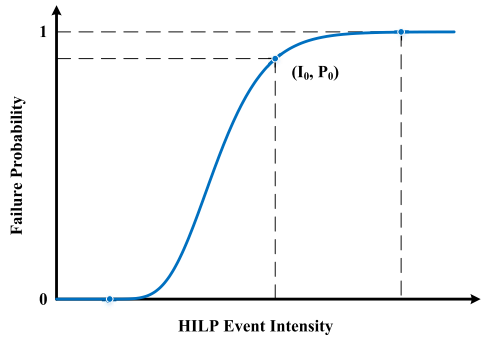

Fig. 4. Illustration of fragility curve of a component.

E. Component Fragility and Restoration

In a HILP event, each component in MES has a certain probability of failure; after the event, each failed component is repaired with a certain time. The failure probability is obtained by the fragility curve of each component, as illustrated in Fig. 4, which presents the relationship between the failure probability of component and the intensity of a HILP event. The component fragility curves are usually represented using lognormal distributions and fitted using empirical data. As for the restoration of failed components, the downtime of each component is considered to be normally distributed. The parameters of distribution of component downtime is decided by the type of component and its damage stage.

III. RESILIENCE ORIENTED PLANNING METHOD

This section presents the proposed resilience-oriented planning method of distribution level MES. First, the quantification of resilience and classification of HILP events are introduced. Then, the generation of scenarios is introduced. Finally, the formulation of the proposed planning optimization problem is presented.

A. Quantification of Resilience

Resilience is the capability to anticipate, absorb, adapt to, and rapidly recover from a HILP event. Analysis of resilience puts particular emphasis on not only the extreme events having high impact on system performance but also the time-varying characteristics of system performance. The concept of resilience covers multiple states before, during and after a HILP event. Fig. 5 shows a system resilience curve across multiple states, described by the time-varying characteristics of system performance before, during and after a HILP event. System performance can be expressed and quantified by different indicators, e.g., the amount of load actually served and the number of operating feeder lines. The system performance goes through five phases, i.e., pre-event state, event unfolding state, post-event state, restorative state, and post-restoration state, before, during and after a HILP event. The system performance in the pre-event state is SP_0 before the HILP event occurs at t_0. During the event unfolding state, the system performance drops from SP_0 to SP_e due to the shock of HILP event. Following the HILP event, the system enters the

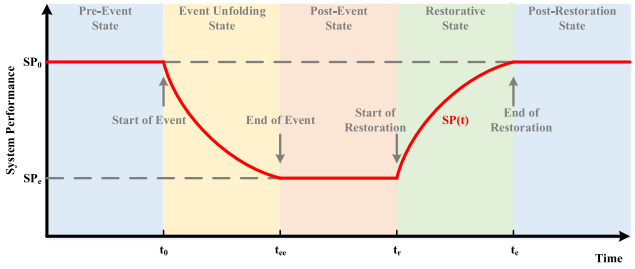

Fig. 5. System resilience curve across multiple states before, during and after a HILP event.

post-event state at t_{ee} and resides in this state for some time before the restoration is initiated at t_r. The system then enters the restorative state, where the system performance recovers from SP_e to SP_0 with the application of restorative actions. Once the restoration is completed at t_e, the system enters the post-restoration state. The time scale of event unfolding state mainly depends on the type of HILP event, e.g., an earthquake usually lasts from seconds to minutes while a typhoon can last from hours to days. The time scale of post-event state mainly depends on the response time of restorative actions, which usually lasts from seconds to hours. The time scale of restorative state mainly depends on the types of failed components and their damage states. A restoration of a failed component can last from hours to more than a week. It should be noted that the curves in the event unfolding state and restorative state shown in Fig. 5 are used for demonstration purposes. Practically, these curves can have any shape depending on the system infrastructure and the impact of HILP event.

According to Fig. 5, different indices can be calculated to quantify the system resilience [7]. In this paper, the total loss of system performance across multiple states during and after a HILP event is used to quantify the resilience of energy supply in MES:

$$\text{Resilience Index} = \int_{t_0}^{t_e} (SP_0 - SP(t))dt \tag{10}$$

It should be noted that this integral covers the restorative state because rapid restoration is also important to a highly-resilient system. It is thought that the system does not totally recover from a HILP event until system performance returns to the initial level before the event. Further, the amount of load actually served is used to describe the system performance in this paper; therefore, the resilience index is equal to the total energy-not-served (ENS) during and after a HILP event:

$$\text{Resilience Index} = \text{ENS} = \int_{t_0}^{t_e} LS(t)dt \tag{11}$$

where LS is the amount of load shedding. It should be noted that the comfort zone of indoor temperature is taken into consideration when calculating the LS of heat/cooling load, through using the equivalent heat/cooling storage device.

Considering the thermal inertia of heat/cooling loads, some loads may not be restored in time even if all failed energy infrastructures are repaired after a HILP event, as shown in Fig. 2. The resilience index is approximated by a coefficient α_{inertia}:

$$\text{Resilience Index} = \int_{t_0}^{t_e} LS(t)dt = \alpha_{\text{inertia}} \cdot \int_{t_0}^{t'_e} LS(t)dt \tag{12}$$

where t'_e is the time when all failed energy infrastructures are repaired ($t_e \geq t'_e$).

TABLE II
CLASSIFICATION OF HILP EVENTS FOR HEAT LOAD IN EH SHOWN IN FIG. 1

Level	Impact
I	Medium Scale: one of heat sources[a] fails
II	Large Scale: part of heat sources fail
III	Extra Large Scale: all of heat sources fail; only heat storage device works for emergency

[a]heat sources here denote the energy converters that produce heat

B. Classification of HILP Events

As mentioned above, a preset limit is used to specify the maximum ENS that can be accepted in a HILP event. However, one single preset maximum ENS is not adequate and not proper to cover all HILP events of different degrees. A stricter limit can be set for a less severe HILP event, while a looser limit can be set for a more severe HILP event. The severity of a HILP event can be judged by the number of failed units or disconnected units that it causes. Taking the EH shown in Fig. 1 as an example, a HILP event can be classified into different levels for the heat load, as shown in Table II. A loosest limit of ENS of heat load is set for a HILP event of level III while a strictest one for that of level I.

As a result, the preset limit of ENS of a certain load is a function of the HILP event impact.

C. Scenario Generation

Both normal operation scenarios and HILP event scenarios are used to perform the planning. The normal operation scenarios are used to estimate the operating cost of MES, while the HILP event scenarios are used to calculate the resilience index.

1) Normal Operation Scenarios: The normal operation scenarios are represented by several typical scenarios of different seasons. The method of scenario reduction, e.g., k-means clustering, is used to characterize load scenarios and RES output scenarios by different patterns for several selected days belonging to different seasons.

2) HILP Event Scenarios: A number of scenarios representing different HILP events are generated beforehand to support the quantification of system resilience. The main steps of scenario generation are:

*Step 1:*Decide the greatest intensity of the studied HILP events, e.g., a once-in-a-century event is considered at most, which depends on the budget of decision makers.

Step 2: Calculate the failure probability of each component in MES according to its fragility curve and the greatest intensity of HILP events decided in Step 1.

Step 3: Sample the status of each component, i.e., operating or failure, in the HILP event according to its failure probability obtained in Step 2.

Step 4: Sample the downtime (restoration time) of each failed component from its corresponding normal distribution of downtime.

Step 5: Combine the sampling results of all components in MES to form a complete HILP event scenario. The total time of a scenario is decided by the longest downtime of failed components.

Step 6: Repeat Step 3 to Step 5 until the number of generated scenarios reaches a preset amount.

In addition, the annual load curves and annual RES output curves are used to present the fluctuations of load and RES output, respectively, in HILP event scenarios.

It should be noted that the impact of a HILP event is considered to be comprised of only one main shock that lasts very short time in this paper, and continuous shocks and cascading failures are not considered.

D. Optimization Problem

A stochastic optimization problem is solved to determine the optimal configuration of distribution level MES. The decision variables include capacities of energy converters, energy storage devices, renewable energy sources and energy feeders (including power feeder lines, gas pipelines and hot water pipelines). If the obtained optimal capacity of some component is zero, this component is not recommended to be invested. The objective of the proposed planning problem is to minimize the sum of equivalent annual capital cost and annual operating cost of the studied MES:

$$\min \left\{ \begin{array}{l} \sum\limits_{i\in\Omega_c} \left[C_i \cdot p_i^c \cdot \frac{r\cdot(1+r)^{\tau_i}}{(1+r)^{\tau_i}-1} \right] + \\ \sum\limits_{s\in\Omega_s} D\cdot\omega(s)\cdot \left\{ \sum\limits_{k\in\Omega_k}\sum\limits_{t=1}^{T} \left[P_k^{in}(t)\cdot\Delta t\cdot c_k^o(t) \right] \right\}\Big|_s \end{array} \right\} \tag{13}$$

where C_i is capacity of component i, p_i^c is unit investment cost of component i, τ_i is lifetime of component i, r is annual interest rate, D is total number of days in one year, $\omega(s)$ is probability of scenario s, T is total number of time periods in one day, $P_k^{in}(t)\cdot\Delta t$ is the amount of energy of type k (e.g., electricity and natural gas) purchased from external energy infrastructures in time period t, $c_k^o(t)$ is price of energy of type k in time period t, and Ω_c, Ω_s and Ω_k are set of candidate components, scenarios and types of import energy, respectively.

The first line of (13) is the equivalent annual capital cost which is calculated by multiplying the net present value of capital cost by a capital recovery factor, while the second line of (13) is the annual operating cost for purchasing energy which is proportional to the weighted mean of operating cost of each scenario. It should be noted that the calculated annual operating cost is only contributed by normal operation scenarios, that is, it does not include the operating costs in HILP events and restorative periods, because: 1) during HILP events, the security of energy supply is far more important than its economy, and 2) the probability of HILP events is too low to be accounted in the annual operating cost.

The constraints of the proposed planning problem consist of two categories, i.e., 1) normal operation constraints, and 2) resilient operation constraints in HILP events.

1) Normal Operation Constraints: This category of constraints is applied to normal operation scenarios where all of the components (including energy converters, energy storage devices, renewable energy sources and energy feeders) in the system are in normal operating state. Normal operation constraints include power conservation constraint, energy converter operating characteristics, energy storage device operating characteristics, energy feeder power loss, component capacity constraint, and energy purchase constraint. Specifically:

a) Power Conservation Constraint: For each unit, including energy converter, energy storage device and renewable energy source, its input power is equal to the sum of receiving end power of its input energy feeders, and its output power is equal to the sum of sending end power of its output energy feeders. For each bus, the sum of input power is equal to that of output power.

$$P_i^{in}(t) = \sum_{j\in\Omega_i^{in}} P_j^{l,out}(t), \forall i\in\Omega_u, \forall t \tag{14}$$

$$P_i^{out}(t) = \sum_{j\in\Omega_i^{out}} P_j^{l,in}(t), \forall i\in\Omega_u, \forall t \tag{15}$$

$$\sum_{j\in\Omega_b^{in}} P_j^{l,in}(t) = \sum_{j\in\Omega_b^{out}} P_j^{l,out}(t), \forall b\in\Omega_b, \forall t \tag{16}$$

where $P_i^{in}(t)$ and $P_i^{out}(t)$ are the input and output power of unit i in time period t, respectively, $P_j^{l,in}(t)$ and $P_j^{l,out}(t)$ are the sending end and receiving end power of energy feeder j in time period t, respectively, Ω_i^{in} and Ω_i^{out} are sets of input and output energy feeders of unit i, respectively, Ω_b^{in} and Ω_b^{out} are sets of input and output energy feeders of bus b, respectively, and Ω_u and Ω_b are set of units and buses, respectively.

b) Energy Converter Operating Characteristics: A energy conversion efficiency is used to model the relationship between the input and output of an energy converter.

$$P_i^{out}(t) = P_i^{in}(t)\cdot\eta_i, \forall i\in\Omega_{uc}, \forall t \tag{17}$$

where η_i is the energy conversion efficiency of energy converter i, and Ω_{uc} is set of energy converters.

For single-input and multi-output energy converters, e.g., CHP, more than one energy conversion efficiency is introduced:

$$P_{CHP}^p(t) = P_{CHP}^g(t)\cdot\eta_{g2p}, \forall t \tag{18}$$

$$P_{CHP}^h(t) = P_{CHP}^g(t)\cdot\eta_{g2h}, \forall t \tag{19}$$

where η_{g2p} and η_{g2h} are efficiencies of gas-power conversion and gas-heat conversion, respectively.

c) Energy Storage Device Operating Characteristics: Besides charging and discharging power, state-of-charge is also introduced to describe the operation of energy storage devices.

$$E_i\cdot(SOC_i(t+1) - SOC_i(t))$$

$$= (P_i^{char}(t) \cdot \eta_i^{char} - P_i^{disch}(t)/\eta_i^{disch}) \cdot \Delta t, \forall i \in \Omega_{us}, \forall t \tag{20}$$

where E_i is the energy capacity of energy storage device i, $SOC_i(t)$ is the state-of-charge of energy storage device i in time period t, $P_i^{char}(t)$ and $P_i^{disch}(t)$ are the charging and discharging power of energy storage device i in time period t, respectively, η_i^{char} and η_i^{disch} are charging and discharging efficiencies of energy storage device i, respectively, and Ω_{us} is set of energy storage devices.

d) Energy Feeder Power Loss: A efficiency coefficient is introduced to model the power loss of energy feeders.

$$P_j^{l,out}(t) = P_j^{l,in}(t) \cdot \eta_j^l, \forall j \in \Omega_l \tag{21}$$

where η_j^l is the efficiency coefficient to model the power loss of energy feeders, and Ω_l is set of energy feeders.

e) Component Capacity Constraint: The operating point of each component, including energy converter, energy storage device, renewable energy source and energy feeder, is constrained by its power capacity or energy capacity.

$$0 \le P_i(t) \le C_i, \forall i \in \Omega_c/\Omega_{ur}, \forall t \tag{22}$$

$$0 \le P_i(t) \le C_i \cdot PU_i(t), \forall i \in \Omega_{ur}, \forall t \tag{23}$$

$$0 \le E_i \cdot SOC_i(t) \le E_i, \forall i \in \Omega_{us}, \forall t \tag{24}$$

where Ω_{ur} is set of renewable energy sources, and PU_i is the per-unit output curve of renewable energy source i.

f) Energy Purchase Constraint: The amount of purchased energy is constrained by the energy supply capacities of external energy infrastructures.

$$0 \le P_k^{buy}(t) \cdot \Delta t \le P_k^{buy,\max}(t) \cdot \Delta t, \forall k \in \Omega_k, \forall t \tag{25}$$

where $P_k^{buy}(t) \cdot \Delta t$ is the amount of purchased energy of type k in time period t, and $P_k^{buy,\max}(t) \cdot \Delta t$ is the upper limit of amount of purchased energy of type k in time period t.

2) Resilient Operation Constraints in HILP Events: This category of constraints is applied to HILP event scenarios. It should be noted that power conservation constraint and energy purchase constraint are also applied to HILP event scenarios; Constraints of component operating characteristics are also applied to normally operating components in HILP event scenarios. Resilient operation constraints in HILP events include component failure constraint, model of pipe energy storage, model of thermal inertia of heat/cooling load, and resilience index constraint. Specifically:

a) Component Failure Constraint: The operating point of each component is also constrained by its status, i.e., operating or failure.

$$0 \le P_i(t) \le M \cdot S_i(t), \forall i \in \Omega_i, \forall t \tag{26}$$

where M is a positive large number, and $S_i(t)$ is the status of component i in time period t, which is determined by sampling.

b) Model of Pipe Energy Storage: If a heat source fails and its downstream hot water pipelines survive in an HILP event, the downstream hot water pipe network is equivalent to a heat storage tank for emergency heat supply; so does cooling network. For details, see Section II.

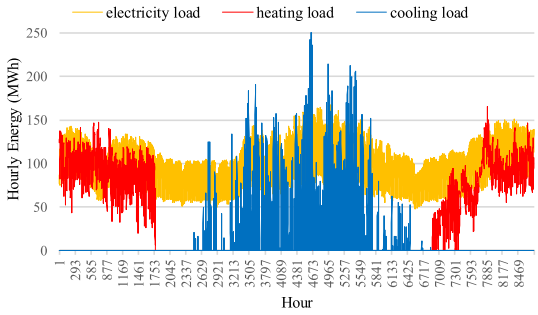

Fig. 6. Annual electricity, heat and cooling load profiles in Tongzhou subsidiary administrative center.

c) Model of Thermal Inertia of Heat/Cooling Load: Equivalent energy storage devices are introduced to model the thermal inertia of heat/cooling load. For details, see Section II.

d) Resilience Index Constraint: The obtained resilience index, i.e., ENS, of each load in each scenario should be less than a preset limit.

$$ENS_k(s) \le \varepsilon_k, \forall k \in \Omega_{load}, \forall s \tag{27}$$

where $ENS_k(s)$ is the ENS of load k in scenario s, ε_k is the preset limit of ENS of load k, and Ω_{load} is set of loads. The ε_k, serving as resilience requirement, is reasonably set to guarantee continuous supply of essential load in HILP events. According to the classification of HILP events, the ε_k is a function of both k and the vector of component status at the end of a HILP event (denoted by $\mathbf{S}_c$):

$$\varepsilon_k = f(k, \mathbf{S}_c) \tag{28}$$

The proposed planning problem is a linear programming (LP) problem which can be efficiently solved by commercial LP solvers.

IV. Case Study

This section conducts a case study of planning of distribution level MES using the proposed resilience-oriented planning method. The impacts of new issues in MES, e.g., energy storage of pipe network, and thermal inertia of heat/cooling load, are studied.

A. Basic Settings

The proposed planning method is used to determine the configuration of the typical distribution level MES that is shown in Fig. 1. The studied MES operates to satisfy electricity load with a peak load of 168 MW, heat load with a peak load of 166 MW, and cooling load with a peak load of 251 MW. Fig. 6 shows the annual electricity, heat and cooling load profiles which refer to Tongzhou subsidiary administrative center, Beijing, China. Roof photovoltaic (PV) system, one kind of RES, is considered as an alternative electricity resource of the studied MES besides main grid electricity. The maximum installed capacity of roof PV system within the area of the studied MES is 50 MW. Fig. 7 shows the hourly PV system output data in Beijing (for 50

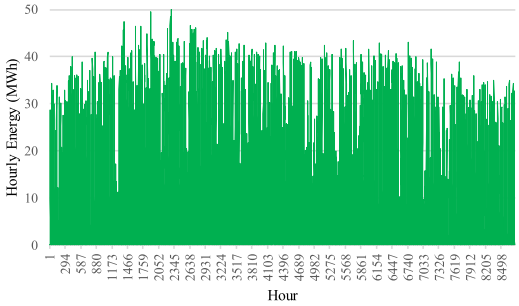

Fig. 7. Hourly PV system output data in Beijing.

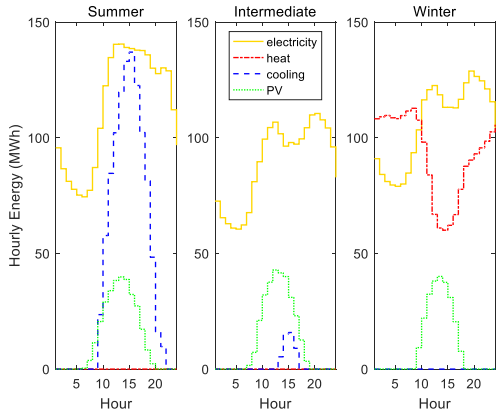

Fig. 8. Selected representative load scenarios and PV system output scenarios in Tongzhou subsidiary administrative center.

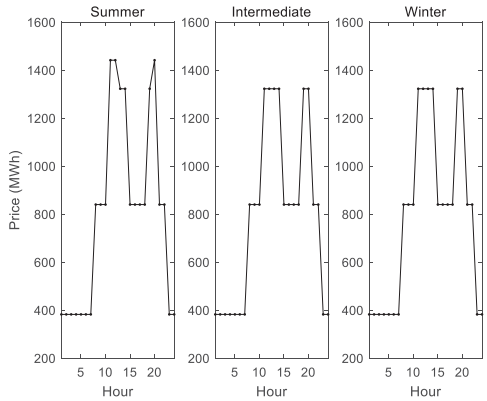

Fig. 9. Curve of electricity price in Beijing.

TABLE III
ENERGY EFFICIENCY, UNIT INVESTMENT COST AND LIFETIME OF CANDIDATE COMPONENTS

	Energy efficiency	Unit investment cost	Lifetime
CHP	El.: 0.3 Therm.: 0.45	7900 CNY/kW	30 year
AB	0.8	851 CNY/kW	20 year
EHP	3	1200 CNY/kW	20 year
CERG	3	1200 CNY/kW	20 year
WARG	0.7	1228 CNY/kW	20 year
HS	Char./ Disch.: 0.9	90 CNY/kWh	20 year
CS	Char./ Disch.: 0.9	190 CNY/kWh	20 year
PV	-	7215 CNY/kW	30 year
Power feeder	0.9	400 CNY/kW	30 year
Water pipeline	0.9	4800 CNY/kW[a]	30 year

[a]Investment cost of water pipeline considers both supply pipe and return pipe.

MW system), which are obtained from the National Renewable Energy Laboratory (NREL) [40].

The normal operation scenarios are represented by several typical scenarios of different seasons to estimate the annual operating cost of the studied MES. Using method of scenario reduction, e.g., k-means clustering, load scenarios and PV system output scenarios are characterized by different patterns for three selected days belonging to summer, intermediate and winter seasons, respectively. The selected representative load scenarios and PV system output scenarios (for 50 MW system) in Tongzhou subsidiary administrative center are shown in Fig. 8.

The price of main grid electricity in Beijing is categorized into peak, flat and valley time prices (1322.2 CNY/MWh, 839.5 CNY/MWh and 381.8 CNY/MWh, respectively). In summer, critical peak price (1440.9 CNY/MWh) is applied to three hours (11:00∼13:00 and 20:00∼21:00) each day. The curve of electricity price in Beijing is shown in Fig. 9. The price of natural gas for industrial and commercial use in Beijing is 300 CNY/MWh. The amount of purchased electricity/natural gas is no more than 250 MWh per hour.

The technological and economic parameters of candidate components, including energy efficiency, unit investment cost and lifetime, are listed in Table III. CHP and AB are built near natural gas bus. EHP, CERG and RES are built near electricity bus. WARG are built near heat bus. The length of corresponding branches, e.g., the branch between CHP and natural gas bus, is assumed to be zero. The length of the rest branches is assumed to be 10 km. The discharge time of HS and CS is 6 hours when operating under rated condition. As for equivalent energy storage, suppose: 1) The energy stored in each pipeline is able to support a 6-hour emergency supply at rated flow rate, if it survives in the HILP event. 2) When heat sources fail to satisfy the heat load, it takes 2 hours for the performance (temperature) of heat load to change from set point to an unacceptable value. Besides, α_{inertia} is assumed to be 1.1.

500 HILP scenarios are considered in the planning to ensure the resilience of the obtained configuration of the studied MES. The greatest intensity of the considered HILP events is determined and, as a result, the failure probabilities of nodes (e.g., energy converters, energy storage devices and RES) and branches (e.g., power feeders, hot/cold water pipelines and natural gas pipelines) in the studied MES are 0.4 and 0.6, respectively. The extreme scenarios, e.g., all the energy sources in MES fail in a HILP event, are neglected because their probabilities are extremely low. The expectation of repair time of failed nodes and branches is 48 hours and 24 hours, respectively, with a standard deviation of 4 hours. The repair time of each failed component is not less than 12 hours. Table IV presents the resilience requirement, i.e., maximum ENS, of each load under HILP events of different levels. It should be noted that the settings of resilience requirement depend on the amount of nonessential load and corresponding maximum tolerable downtime.

TABLE IV
RESILIENCE REQUIREMENT OF EACH LOAD UNDER HILP EVENTS OF DIFFERENT LEVELS

Load	Level	Resilience requirement
Electricity load	-	10 MWh
Heat load	I	10 MWh
	II	200 MWh
	III	500 MWh
Cooling load	I	10 MWh
	II	100 MWh

TABLE V
PLANNING SCHEMES AND CORRESPONDING ANNUAL COST GIVEN BY DIFFERENT PLANNING METHODS

	The Proposed Planning Method	Alternative Planning Method I	Alternative Planning Method II	Alternative Planning Method III
CHP	225 MW	225 MW		
AB	280 MW	356 MW		
EHP	137 MW	117 MW		
CERG	110 MW	92 MW		
WARG	199 MW	309 MW	No Feasible Solution	No Feasible Solution
HS	235 MWh	300 MWh		
CS	3 MWh	89 MWh		
PV	50 MW	50 MW		
Annual Cost	2.01 Billion CNY	2.14 Billion CNY		

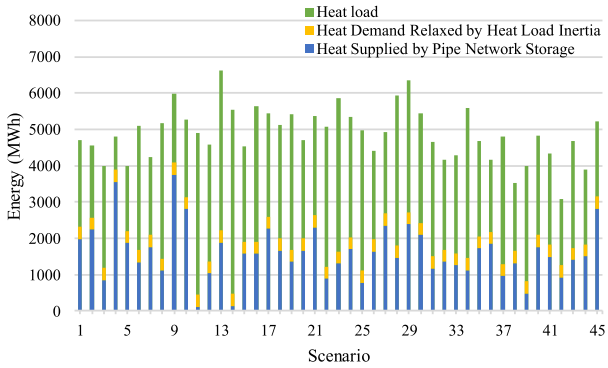

Fig. 10. Heat supplied by pipe network storage and heat demand relaxed by heat load inertia in 45 HILP events in winter season.

TABLE VI
RELAXED RESILIENCE REQUIREMENT OF EACH LOAD UNDER HILP EVENTS OF DIFFERENT LEVELS

Load	Level	Resilience requirement
Electricity load	-	100 MWh
Heat load	I	100 MWh
	II	4000 MWh
	III	5000 MWh
Cooling load	I	2000 MWh
	II	2500 MWh

B. Results and Discussion

To show and analyze the impact of energy storage of pipe network and thermal inertia of heat/cooling load, another three planning methods besides the proposed one are used to determine the configuration of MES shown in Fig. 1. Specifically:

1) The proposed planning method. Both energy storage of pipe network and thermal inertia of heat/cooling load are considered.
2) Alternative planning method I. Energy storage of pipe network is considered; Inertia of heat/cooling load is neglected.
3) Alternative planning method II. Energy storage of pipe network is neglected; Inertia of heat/cooling load is considered.
4) Alternative planning method III. Both energy storage of pipe network and thermal inertia of heat/cooling load are neglected.

Under the resilience requirement that is shown in Table IV, the planning schemes and corresponding annual cost given by these four planning methods are presented in Table V. The capacities of power feeders and water pipelines are determined by the planned capacities of energy converters and energy storage devices. Alternative planning method II and III suggest that no planning scheme can satisfy the resilience requirement shown in Table IV. Alternative planning method II and III do not use the energy stored in the pipe network, which is a significant buffer against energy shortage in HILP events. Without this buffer provided by pipe network, the resilience of the studied MES is limited to a relatively low level. Under the planning scheme obtained by the proposed planning method, the heat supplied by pipe network storage in 45 HILP events in winter season is calculated and shown in Fig. 10; On average, the heat provided by pipe network storage accounts for 33.0% of heat load in these HILP events. Comparing the planning results of the proposed planning method and alternative planning method I, the capacities of AB, WARG, HS and CS are significantly reduced due to thermal inertia of heat/cooling load. This thermal inertia relaxes the constraint of instantaneous power balance, and thus reduce the demand for energy supply in HILP events. Similarly, under the planning scheme obtained by the proposed planning method, the heat demand relaxed by heat load inertia in 45 HILP events in winter season is calculated and shown in Fig. 10; On average, the heat demand relaxed by heat load inertia accounts for 6.8% of heat load in these HILP events. The capacities of EHP and CERG obtained by the proposed planning method are slightly larger in order to consume surplus electricity generated by CHP. Under the same resilience requirement, the proposed planning method reduces equivalent annual cost, including capital cost and operating cost, by about 6%.

To further conduct a comparison among the four planning methods, the resilience requirement shown in Table IV is relaxed, as shown in Table VI.

Under the relaxed resilience requirement shown in Table VI, the planning schemes and corresponding annual cost given by these four planning methods are presented in Table VII. With looser resilience requirement (comparing Table VII with Table V), the capacities of energy converters and energy storage devices are reduced, and equivalent annual cost decreases. Using either emergency energy storage of pipe network or thermal inertia of heat/cooling load, the invested capacity of each energy converter or energy storage device can be reduced when

TABLE VII
PLANNING SCHEMES AND CORRESPONDING ANNUAL COST GIVEN BY DIFFERENT PLANNING METHODS

	The Proposed Planning Method	Alternative Planning Method I	Alternative Planning Method II	Alternative Planning Method III
CHP	150 MW	133 MW	207 MW	203 MW
AB	73 MW	92 MW	100 MW	148 MW
EHP	18 MW	26 MW	70 MW	99 MW
CERG	53 MW	58 MW	86 MW	84 MW
WARG	43 MW	59 MW	169 MW	241 MW
HS	0	0	298 MWh	323 MWh
CS	0	20 MWh	55 MWh	118 MWh
PV	50 MW	50 MW	50 MW	50 MW
Annual Cost	1.41 Billion CNY	1.44 Billion CNY	1.83 Billion CNY	1.99 Billion CNY

TABLE VIII
PLANNING SCHEMES AND CORRESPONDING ANNUAL COST AND EENS GIVEN BY DIFFERENT PLANNING METHODS

	With Classification of HILP Events	Without Classification of HILP Events	Comparison[a]
CHP	225 MW	225 MW	0
AB	280 MW	213 MW	-24%
EHP	137 MW	155 MW	+13%
CERG	110 MW	115 MW	+4%
WARG	199 MW	179 MW	-10%
HS	235 MWh	235 MWh	0
CS	3 MWh	3 MWh	0
PV	50 MW	50 MW	0
Annual Cost	2.012 Billion CNY	2.006 Billion CNY	-0.3%
$EENS_e$	9 MWh	9 MWh	0
$EENS_h$	108 MWh	187 MWh	+73%
$EENS_c$	19 MWh	34 MWh	+74%

[a]This column calculates the difference between the two groups of planning results. The results given by the proposed planning method considering classification of HILP events serves as the benchmark.

meeting the same resilience requirement shown in Table VI. Especially, the proposed planning method suggests that HS and CS are not necessary to be invested under such loose resilience requirement. Compared to alternative planning method III, the proposed planning method reduces equivalent annual cost by about 29%.

The advantages of classification of HILP events in the proposed planning method is proved. Table VIII shows planning schemes and corresponding annual cost and expected ENS (EENS) obtained by the proposed planning method with and without classification of HILP events. Under the circumstances where classification of HILP events is considered, the resilience requirement shown in Table IV is used; Under the circumstances where classification of HILP events is not considered, only one single limit of resilience index is set for each energy sector regardless of intensity of HILP events (Specifically, 10 MWh for electricity load, 500 MWh for heat load and 100 MWh for cooling load). EENS presented in Table VIII is the expected energy not supplied in one HILP event. The subscripts e, h and c of EENS indicate electricity, heat and cooling loads, respectively. Not considering classification of HILP events means only being concerned with the impacts of HILP events of relatively high intensity level. The relaxation of resilience requirement in HILP events of relatively low intensity level leads to lower annual cost and higher EENS in HILP events. For example, as Table VIII shows, annual cost is reduced by 0.3% while EENS of heat and cooling loads are increased by 73% and 74%, respectively. Annual cost is mainly impacted by the resilience requirement in relatively severer HILP events; therefore, stricter resilience requirement in relatively less severe HILP events does not cause a significant increase in annual cost while it contributes to a great improvement in EENS of loads.

TABLE IX
TWO GROUPS OF RESILIENCE REQUIREMENT UNDER HILP EVENTS OF DIFFERENT LEVELS

Load	Level	Resilience requirement	
		Maximum amount of ENS (for the proposed planning method)	Maximum amount of load shedding (for alternative planning method IV)
Electricity load	-	10 MWh	5 MW
Heat load	I	10 MWh	5 MW
	II	200 MWh	100 MW
	III	500 MWh	150 MW
Cooling load	I	10 MWh	5 MW
	II	100 MWh	50 MW

To study the impact of the definition of resilience index on the planning results, two planning methods are compared:

1) The proposed planning method, where the resilience index is defined as the amount of ENS in a HILP event.
2) Alternative planning method IV, where the resilience index is defined as the maximum amount of load shedding in a HILP event.

Table IX shows two groups of resilience requirement that are set for these two planning methods. Based on the given resilience requirement, the planning schemes and corresponding system security indices given by these two planning methods are shown in Table X. The presented system security indices include the EENS, the maximum amount of load shedding (denoted by $LS_{\max}$), and the expected length of time that the load is in short supply in a HILP event (denoted by EST). The subscripts e, h and c of these indices indicate electricity, heat and cooling loads, respectively. Compared to the proposed planning method, alternative planning method IV reduces the maximum amount of load shedding by up to 50%. Although alternative planning method IV has advantages in directly limiting the instantaneous load shedding, it does not take into consideration the length of time that the load is in short supply. As a result, alternative planning method IV leads to much larger EENS and EST than the proposed planning method. For example, the $EENS_e$ and EST_e caused by alternative planning method IV are about 19 and 39 times as large as the $EENS_e$ and EST_e caused by the proposed planning method, respectively. The proposed planning method limits the amount of ENS to achieve a balance between limiting the instantaneous load shedding and limiting the length of time that the load is in short supply.

TABLE X
PLANNING SCHEMES AND CORRESPONDING SYSTEM SECURITY INDICES GIVEN BY DIFFERENT PLANNING METHODS

	The Proposed Planning Method	Alternative Planning Method IV	Comparison[a]
CHP	225 MW	167 MW	-26%
AB	280 MW	3 MW	-99%
EHP	137 MW	110 MW	-20%
CERG	110 MW	117 MW	+6%
WARG	199 MW	157 MW	-21%
HS	235 MWh	0	-100%
CS	3 MWh	31 MWh	933%
PV	50 MW	50 MW	0
Annual Cost	2.01 Billion CNY	1.68 Billion CNY	-16%
$EENS_e$	9 MWh	175 MWh	+1844%
$EENS_h$	108 MWh	1061 MWh	+882%
$EENS_c$	19 MWh	103 MWh	+442%
$LS_{max,\,e}$	10 MW	5 MW	-50%
$LS_{max,\,h}$	162 MW	150 MW	-7%
$LS_{max,\,c}$	91 MW	50 MW	-45%
EST_e	0.9 Hours	35 Hours	+3789%
EST_h	1.7 Hours	13 Hours	+665%
EST_c	0.8 Hours	4 Hours	+400%

[a]This column calculates the difference between the two groups of planning results. The results given by the proposed planning method serves as the benchmark.

V. CONCLUSION

This paper proposes a resilience-oriented planning method to determine optimal configuration of distribution level MES, e.g., urban energy supply systems, considering comprehensive impacts from supply, network and demand sides in MES. Impacts of energy shifting at supply side, pipe storage at network side and thermal inertia at demand side are described in the same linear modeling framework using EH model. Generalized energy storage resources including centralized and distributed energy storage devices, pipe network storage and building heat capacity are all modeled into centralized energy storage to facilitate an efficient configuration planning of MES. In the case study, the proposed planning method is used to determine the configuration of typical distribution level MES, which contains energy converters, energy storage devices, renewable energy sources and heat/cooling pipe network, to satisfy electricity, heat and cooling loads in Tongzhou subsidiary administrative center, Beijing, China. Using either emergency energy storage of pipe network or thermal inertia of heat/cooling load, the invested capacity of each energy converter or energy storage device can be reduced when meeting the same resilience requirement, thus further reducing equivalent annual cost of MES. Classification of HILP events is used in the proposed planning method. It is proved that classification of HILP events can contribute to a great improvement in EENS of loads without causing a significant increase in annual cost.

REFERENCES

[1] R. Moreno *et al.*, "From reliability to resilience: Planning the grid against the extremes," *IEEE Power Energy Mag.*, vol. 18, no. 4, pp. 41–53, Jul./Aug. 2020.

[2] M. Panteli and P. Mancarella, "The grid: Stronger, bigger, smarter?: Presenting a conceptual framework of power system resilience," *IEEE Power Energy Mag.*, vol. 13, no. 3, pp. 58–66, May/Jun. 2015.

[3] M. Panteli, D. N. Trakas, P. Mancarella, and N. D. Hatziargyriou, "Power systems resilience assessment: Hardening and smart operational enhancement strategies," *Proc. IEEE*, vol. 105, no. 7, pp. 1202–1213, Jul. 2017.

[4] Z. Bie, Y. Lin, G. Li, and F. Li, "Battling the extreme: A study on the power system resilience," *Proc. IEEE*, vol. 105, no. 7, pp. 1253–1266, Jul. 2017.

[5] P. Mancarella, "MES (multi-energy systems): An overview of concepts and evaluation models," *Energy*, vol. 65, pp. 1–17, Feb. 2014.

[6] M.-H. Shariatkhah *et al.*, "Modeling the reliability of multi-carrier energy systems considering dynamic behavior of thermal loads," *Energy Build*, vol. 103, pp. 375–383, Sep. 2015.

[7] M. Panteli, P. Mancarella, D. N. Trakas, E. Kyriakides, and N. D. Hatziargyriou, "Metrics and quantification of operational and infrastructure resilience in power systems," *IEEE Trans. Power Syst.*, vol. 32, no. 6, pp. 4732–4742, Nov. 2017.

[8] S. Espinoza, A. Poulos, H. Rudnick, J. C. de la Llera, M. Panteli, and P. Mancarella, "Risk and resilience assessment with component criticality ranking of electric power systems subject to earthquakes," *IEEE Syst. J.*, vol. 14, no. 2, pp. 2837–2848, Jun. 2020.

[9] A. Gholami, T. Shekari, M. H. Amirioun, F. Aminifar, M. H. Amini, and A. Sargolzaei, "Toward a consensus on the definition and taxonomy of power system resilience," *IEEE Access*, vol. 6, pp. 32035–32053, 2018.

[10] Y. Wang, C. Chen, J. Wang, and R. Baldick, "Research on resilience of power systems under natural Disasters—A review," *IEEE Trans. Power Syst.*, vol. 31, no. 2, pp. 1604–1613, Mar. 2016.

[11] D. N. Trakas and N. D. Hatziargyriou, "Resilience constrained day-ahead unit commitment under extreme weather events," *IEEE Trans. Power Syst.*, vol. 35, no. 2, pp. 1242–1253, Mar. 2020.

[12] M. Yan *et al.*, "Enhancing the transmission grid resilience in ice storms by optimal coordination of power system schedule with pre-positioning and routing of mobile DC de-icing devices," *IEEE Trans. Power Syst.*, vol. 34, no. 4, pp. 2663–2674, Jul. 2019.

[13] H. Gao, Y. Chen, S. Mei, S. Huang, and Y. Xu, "Resilience-Oriented pre-hurricane resource allocation in distribution systems considering electric buses," *Proc. IEEE*, vol. 105, no. 7, pp. 1214–1233, Jul. 2017.

[14] G. Huang, J. Wang, C. Chen, J. Qi, and C. Guo, "Integration of preventive and emergency responses for power grid resilience enhancement," *IEEE Trans. Power Syst.*, vol. 32, no. 6, pp. 4451–4463, Nov. 2017.

[15] C. Wang, Y. Hou, F. Qiu, S. Lei, and K. Liu, "Resilience enhancement with sequentially proactive operation strategies," *IEEE Trans. Power Syst.*, vol. 32, no. 4, pp. 2847–2857, Jul. 2017.

[16] Z. Wang and J. Wang, "Self-healing resilient distribution systems based on sectionalization into microgrids," *IEEE Trans. Power Syst.*, vol. 30, no. 6, pp. 3139–3149, Nov. 2015.

[17] F. Hafiz, B. Chen, C. Chen, A. Rodrigo de Queiroz, and I. Husain, "Utilising demand response for distribution service restoration to achieve grid resiliency against natural disasters," *IET Gener. Transmiss. Distrib.*, vol. 13, no. 14, pp. 2942–2950, 2019.

[18] H. Gao, Y. Chen, Y. Xu, and C. Liu, "Resilience-oriented critical load restoration using microgrids in distribution systems," *IEEE Trans. Smart Grid*, vol. 7, no. 6, pp. 2837–2848, Nov. 2016.

[19] B. Chen, Z. Ye, C. Chen, J. Wang, T. Ding, and Z. Bie, "Toward a synthetic model for distribution system restoration and crew dispatch," *IEEE Trans. Power Syst.*, vol. 34, no. 3, pp. 2228–2239, May 2019.

[20] Y. Wang *et al.*, "Dynamic load restoration considering the interdependencies between power distribution systems and urban transportation systems," in *Proc. CSEE J. Power Energy Syst.*, vol. 6, no. 4, pp. 772–781, Dec. 2020.

[21] T. Ding, Z. Wang, W. Jia, B. Chen, C. Chen, and M. Shahidehpour, "Multiperiod distribution system restoration with routing repair crews, mobile electric vehicles, and soft-open-point networked microgrids," *IEEE Trans. Smart Grid*, vol. 11, no. 6, pp. 4795–4808, Nov. 2020.

[22] A. Bagheri, C. Zhao, F. Qiu, and J. Wang, "Resilient transmission hardening planning in a high renewable penetration era," *IEEE Trans. Power Syst.*, vol. 34, no. 2, pp. 873–882, Mar. 2019.

[23] W. Yuan, J. Wang, F. Qiu, C. Chen, C. Kang, and B. Zeng, "Robust optimization-based resilient distribution network planning against natural disasters," *IEEE Trans. Smart Grid*, vol. 7, no. 6, pp. 2817–2826, Nov. 2016.

[24] M. Nazemi, M. Moeini-Aghtaie, M. Fotuhi-Firuzabad, and P. Dehghanian, "Energy storage planning for enhanced resilience of power distribution networks against earthquakes," *IEEE Trans. Sustain. Energy*, vol. 11, no. 2, pp. 795–806, Apr. 2020.

[25] H. Zhang, P. Wang, S. Yao, X. Liu, and T. Zhao, "Resilience assessment of interdependent energy systems under hurricanes," *IEEE Trans. Power Syst.*, vol. 35, no. 5, pp. 3682–3694, Sep. 2020.

[26] M. Bao, Y. Ding, M. Sang, D. Li, and J. Yan, "Modeling and evaluating nodal resilience of multi-energy systems under windstorms," *Appl. Energ.*, vol. 270, 2020, Art. no. 115136.
[27] M. H. Amirioun, F. Aminifar, and M. Shahidehpour, "Resilience-Promoting proactive scheduling against hurricanes in multiple energy carrier microgrids," *IEEE Trans. Power Syst.*, vol. 34, no. 3, pp. 2160–2168, May 2019.
[28] Z. Liang, Q. Alsafasfeh, and W. Su, "Proactive resilient scheduling for networked microgrids with extreme events," *IEEE Access*, vol. 7, pp. 112639–112652, 2019.
[29] M. Yan, Y. He, M. Shahidehpour, X. Ai, Z. Li, and J. Wen, "Coordinated regional-district operation of integrated energy systems for resilience enhancement in natural disasters," *IEEE Trans. Smart Grid*, vol. 10, no. 5, pp. 4881–4892, Sep. 2019.
[30] Y. Lin, B. Chen, J. Wang, and Z. Bie, "A combined repair crew dispatch problem for resilient electric and natural gas system considering reconfiguration and DG islanding," *IEEE Trans. Power Syst.*, vol. 34, no. 4, pp. 2755–2767, Jul. 2019.
[31] C. Shao, M. Shahidehpour, X. Wang, X. Wang, and B. Wang, "Integrated planning of electricity and natural gas transportation systems for enhancing the power grid resilience," *IEEE Trans. Power Syst.*, vol. 32, no. 6, pp. 4418–4429, Nov. 2017.
[32] C. Wang *et al.*, "Robust defense strategy for gas–electric systems against malicious attacks," *IEEE Trans. Power Syst.*, vol. 32, no. 4, pp. 2953–2965, Jul. 2017.
[33] C. He, C. Dai, L. Wu, and T. Liu, "Robust network hardening strategy for enhancing resilience of integrated electricity and natural gas distribution systems against natural disasters," *IEEE Trans. Power Syst.*, vol. 33, no. 5, pp. 5787–5798, Sep. 2018.
[34] C. Lv, H. Yu, P. Li, K. Zhao, H. Li, and S. Li, "Coordinated operation and planning of integrated electricity and gas community energy system with enhanced operational resilience," *IEEE Access*, vol. 8, pp. 59257–59277, 2020.
[35] Z. Guo, G. Li, M. Zhou, and W. Feng, "Resilient configuration approach of integrated community energy system considering integrated demand response under uncertainty," *IEEE Access*, vol. 7, pp. 87513–87533, 2019.
[36] M. Geidl, G. Koeppel, P. Favre-Perrod, B. Klockl, G. Andersson, and K. Frohlich, "Energy hubs for the future," *IEEE Power Energy Mag*, vol. 5, no. 1, pp. 24–30, Jan. 2007.
[37] W. Huang, N. Zhang, J. Yang, Y. Wang, and C. Kang, "Optimal configuration planning of multi-energy systems considering distributed renewable energy," *IEEE Trans. Smart Grid*, vol. 10, no. 2, pp. 1452–1464, Mar. 2019.
[38] T. Xia, W. Huang, X. Lu, N. Zhang, and C. Kang, "Planning district multiple energy systems considering year-round operation," *Energy*, vol. 213, Dec. 2020, Art. no. 118829.
[39] J. Yang, N. Zhang, A. Botterud, and C. Kang, "On an equivalent representation of the dynamics in district heating networks for combined electricity-heat operation," *IEEE Trans. Power Syst.*, vol. 35, no. 1, pp. 560–570, Jan. 2020.
[40] NREL's PVWatts Calculator, National Renewable Energy Laboratory, Golden, CO, USA. Accessed: Apr. 1, 2021. [Online]. Available: http://pvwatts.nrel.gov

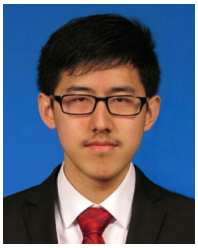

Wujing Huang (Student Member, IEEE) received the B.S. degree in 2017 from the Department of Electrical Engineering, Tsinghua University, Beijing, China, where he is currently working toward the Ph.D. degree.

His research interests include modeling, operation, and planning of multiple energy systems.

Xi Zhang (Member, IEEE) received the B.S. and M.S. degrees in electrical engineering from Tsinghua University, Beijing, China, in 2012 and 2014, respectively, and the Ph.D. degree from Imperial College London, London, U.K., in 2019.

He is currently a Research Associate with Imperial College London. His research interests include whole-energy system planning and multivector energy system modeling.

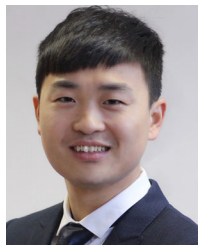

Kangping Li (Member, IEEE) received the B.S. and Ph.D. degrees in electrical engineering from North China Electric Power University, Baoding, China, in 2015 and 2020, respectively.

He is currently a Postdoctoral Researcher with the Department of Electrical Engineering, Tsinghua University, Beijing, China. His research interests include demand response, electricity market, and power system optimization.

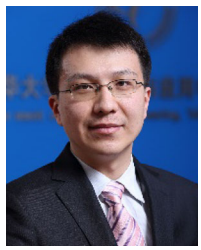

Ning Zhang (Senior Member, IEEE) received the B.S. and Ph.D. degrees from the Department of Electrical Engineering, Tsinghua University, Beijing, China in 2007 and 2012, respectively.

He is currently an Associate Professor with the same university. His research interests include multiple energy systems integration, renewable energy, and power system planning and operation.

Goran Strbac (Member, IEEE) is currently a Professor of electrical energy systems with Imperial College London, London, U.K.

His current research interests include electricity generation, transmission and distribution operation, planning and pricing, and integration of renewable and distributed generation in electricity systems.

Chongqing Kang (Fellow, IEEE) received the Ph.D. degree from the Department of Electrical Engineering, Tsinghua University, Beijing, China, in 1997.

He is currently a Professor with the same university. His research interests include power system planning, power system operation, renewable energy, low carbon electricity technology, and load forecasting.